The Status of Thermophotovoltaic Energy Conversion Technology at Lockheed Martin Corp.

E.J. Brown, P.F. Baldasaro, S.R. Burger, L.R. Danielson, D.M. DePoy, G.J. Nichols, W.F. Topper, T.D. Rahmlow

THE STATUS OF THERMOPHOTOVOLTAIC ENERGY CONVERSION TECHNOLOGY AT LOCKHEED MARTIN CORP.

EJ Brown, PF Baldasaro, SR Burger, LR Danielson, DM DePoy, GJ Nichols, WF Topper
Lockheed Martin Corp.
PO Box 1072   Schenectady, New York 12301
(518) 395-7045; fax 395-6136; email browne@kapl.gov

TD Rahmlow Rugate Technologies, Inc.
353 Christian Street   Oxford, CT 06478
(203) 267-3154; email info@rugate.com

ABSTRACT
 In a thermophotovoltaic (TPV) energy conversion system, a heated surface radiates in the mid-infrared range onto photodiodes which are sensitive at these energies. Part of the absorbed energy is converted into electric output. Conversion efficiency is maximized by reducing the absorption of non-convertible energy with some form of spectral control. In a TPV system, many technology options exist. Our development efforts have concentrated on flat-plate geometries with greybody radiators, low bandgap quaternary diodes, front surface tandem filters and a multi-chip module (MCM) approach that allows selective fabrication processes to match diode performance.

Recently, the authors achieved conversion efficiencies of about 20% (radiator 950°C, diodes 22°C) for a module in a prototypic cavity test environment. These tests employed InGaAsSb diodes with 0.52 eV bandgap and front surface filters for spectral control. This paper provides details of the individual system components and describes the measurement technique used to record these efficiencies.

SUMMARY
Lockheed Martin has been developing thermophotovoltaic (TPV) direct energy conversion for about eight years. Significant progress has been achieved in four key areas:

1. Conversion Efficiency –significant progress has been made in conversion efficiency as shown in Figure 1. The latest modules made with low-bandgap cells and front surface filters are about 20% efficient with a hot side radiator at 950°C and the diodes near room temperature.

2. Spectral Control – efforts to limit the parasitic absorption of non-convertible (below diode bandgap) photons have concentrated on front surface selective filters. The most recent tandem filters have spectral efficiency of 79% (see Figure 2).

3. Prototypic Testing – to carry out direct measurements of integrated TPV systems under prototypic conditions, a photonic cavity test (PCT) system was developed that incorporates all geometric, electrical, optical and photonic effects (see Figure 3). All efficiency results presented here are determined from measurements carried out in the PCT system.

4. Integrated System Modeling – in-house computer models were developed and extensively benchmarked using earlier results obtained in the PCT system (described above). Figure 4 shows the comparison of computer modeling of four modules that were built and tested over the past two years.

BACKGROUND
In a TPV energy conversion system, a heated surface radiates to light-sensitive diodes which convert a portion of the incident energy to electric power as shown in Figure 5. Diodes can only generate electric power from photons with energy greater than the bandgap of the material (see Figure 6). If a photon with energy less than the bandgap is absorbed by the diode, it is converted to waste heat which lowers the

overall conversion efficiency. Because of materials considerations, the radiant surface is usually limited to temperatures between 900-1200°C.

TPV was first proposed in the 1960's (Ref. 1,2,3). Interest waned, however, because the commonly available semiconductor (silicon) had a relatively high bandgap (1.1 eV). Assuming a blackbody radiator at 950°C, only 0.6% of the radiant energy is potentially convertible to electric power. Interest in TPV was revived in the 1990's with the development of compound semiconductors which made possible high quality semiconductors with lower bandgaps. For example, a GaSb diode with a bandgap of 0.73 eV, can convert 8.3% of the radiant energy from a 950°C radiator. For semiconductors with lower bandgaps, an even larger fraction of the radiant spectrum is convertible to electric output.

After the development of lower bandgap semiconductors, one of the critical technical challenges was the creation of a highly efficient spectral control system. Unlike a photovoltaic system, TPV can make significant improvements in efficiency by limiting absorption of non-convertible photons. By tailoring the emission spectrum or selectively reflecting sub-bandgap photons back to the radiator for reabsorption, conversion efficiency can be significantly increased.

SYSTEM TECHNOLOGY OPTIONS

An integrated TPV system is comprised of five critical components; for each component, there are a number of technology options. The choices made will be governed by system performance trade-offs and the specific criteria to which the system is designed. For example, low bandgap diodes tend to be quite expensive but they can yield a significantly higher surface power density. The matrix of design elements and technology options produces a large number of possible system configurations.

Table 1 (below) describes the system elements, technology options and highlights the choices made by Lockheed Martin in designing the systems described in the remainder of this paper.

TABLE 1 -- Technology Options for an Integrated TPV Energy Conversion System
(boldface entries indicate technology options incorporated in Lockheed Martin system)

SYSTEM GEOMETRY	RADIATOR	DIODES	SPECTRAL CONTROL	NETWORK
Flat Plate	**Grey Body**	Silicon	Radiator Treatment	**Multi-chip Assembly**
Cylindrical	Selective Radiator	Binary	Front Surface Filter	**Monolithic Integration***
	Spectral Radiator	Ternary	- Interference	
		Quaternary	- **Tandem**	
	Textured Surface		- Metal Dipole	
		High Bandgap	Back Surface Refl*	
		Low Bandgap	*requires transparent diode for sub-bandgap photons	*LM is developing materials to enable the MIM design using InGaAsSb diodes

2

SYSTEM EFFICIENCY

The overall system conversion efficiency can be viewed as the product of the component performance factors:

$$\eta_{TPV} = \eta_{diode} * \eta_{spectral} * \eta_{mod} \qquad equ.\ 1$$

where η_{diode} and $\eta_{spectral}$ are the separate performance factors for the diodes and (for Lockheed Martin system) front surface spectral control filters. η_{mod} is the factor to account for parasitic photon absorption in gold conduction structures and variations in diode output.

It is this definition of efficiency that is the implicit basis for all measurements carried out on small-scale modules and reported in this paper. Extrapolating results reported here to larger systems would require the application of other factors to accurately model overall conversion efficiency. Some of these are:

> Factor for parasitic photon absorption in cracks between adjacent diodes
> Factor for parasitic photon absorption in cold-side structural members
> Factor for network losses; reduction of electric output due to mismatched diodes
> Factor for inefficiency of the combustion system (if applicable)
> Factor for effect of an inert cover gas (if applicable)
> Factor for power required to run auxiliary systems (air blowers, fuel pumps)
> Factor for lifetime system degradation

It is noted that, while this formulation is a convenient method to conceptualize TPV module behavior, it can be misleading because it appears that the separate factors are independent. In fact, this is often not the case. Efforts to increase η_{mod} by reducing the size of the gold conduction structures, for example, can increase the series resistance which would decrease the diode efficiency through the fill factor. Similarly, if $\eta_{spectral}$ is increased at the expense of short circuit current, a secondary effect will also reduce the open circuit voltage and, therefore, module efficiency as well. This interdependency of efficiency terms is a major reason why reliable measurements of TPV efficiency must be carried out on an integrated module and not synthesized from separate measurements on the individual components.

DIODES

In designing TPV diodes, semiconductor material choice and bandgap selection is governed by the need to balance energy conversion efficiency and surface power density. For a given photonic energy spectrum, a lower bandgap diode material will release more electrons to be collected. However, lower bandgap diode materials have intrinsic properties that decrease their photon to electron conversion efficiency.

The process of selecting the optimum TPV diode bandgap material depends on a particular system's efficiency and power density requirements. Given a specific heat source temperature, diode temperature and spectral control efficiency, a diode bandgap versus TPV system efficiency (η_{TPV}) and power density relationship can be determined as shown in Figure 7. A clear trade-off exists between power density or system efficiency.

Terrestrial heat source TPV systems require diode bandgaps in the range of 0.4 to 0.72 eV. Group III-V semiconductor materials such as the gallium-indium-arsenide (GaInAs), gallium-indium-arsenide-antimonide (GaInAsSb), indium-arsenide-phosphide-antimonide (InAsPSb), and gallium antimonide (GaSb) alloys are attractive candidates since they are direct bandgap materials and can be grown on commercially available substrates.

At Lockheed Martin, we have been focusing on the GaInAsSb alloy system lattice matched to GaSb substrates. The GaInAsSb alloy composition can be varied to obtain an approximate bandgap range of 0.3 to 0.7 eV (ref. 4). We have targeted a low-bandgap (~0.53 eV) material as having the highest potential to maximize power density while maintaining an achievable high efficiency. Figure 8 depicts the GaInAsSb

3

TPV diode layers and metal contacts. The GaInAsSb diode is grown by organo-metallic vapor phase epitaxy (OMVPE) on commercially available n-type GaSb substrates.

The diode efficiency, η_{diode}, is the ratio of the electric power output to the above-bandgap energy absorbed in active areas of the cell. It is actually the product of four other factors:

$$\eta_{diode} = Fo * QEint * [e * (Voc/Eg)] * FF \qquad (Equ. 2)$$

where: Fo is the penalty term to account for the fact that photons with energy significantly above the semiconductor bandgap will generate waste heat with the excess energy

QEint is the average internal quantum efficiency, i.e. the probability that an absorbed photon will result in a charge carrier that is collected at the diode junction

[e * (Voc/Eg)] is the product of the elementary electronic charge times the fraction of the bandgap achieved by the open circuit voltage generated by the diode

FF is the diode fill factor, i.e. the penalty paid because no diode can, at the same time produce the open circuit voltage and the short circuit current. FF is heavily dependent on the series resistance in the diode and connecting structures.

Under prototypic conditions as defined in this paper, the diode efficiency for our latest GaInAsSb cells is:

$$\eta_{diode} = 0.79 * 0.83 * [0.60] * 0.69 \qquad = 0.27$$

Current efforts to improve TPV diode performance are focusing on improving minority carrier lifetimes to improve the voltage factor (Voc/Eg) and quantum efficiency. Minority carrier recombination mechanisms (Auger, shockley-read-hall, and interface recombinations) and their sensitivities to diode parameters (doping type and levels) are being investigated. Incorporation of a back surface reflector is also being studied to assess the advantages of a two-pass architecture and potential gains from photon recycling.

SPECTRAL CONTROL

Spectral control is a key technology for TPV direct energy conversion systems. As shown in Figure 6, for blackbody radiator at 950°C with 0.52 eV bandgap diodes, only ~25% of the incident radiation can be converted to electricity. The remaining ~75% of the incident radiation cannot be converted to electricity, and, therefore, would be parasitically absorbed if no steps were taken.

Lockheed Martin has favored selective front-surface selective filters for spectral control because, unlike special radiator techniques, they operate at about room temperature (Ref. 5). Furthermore, it is convenient to separate the spectral control function from the diode because the ability to optimize the performance of each component separately.

The goal for TPV spectral control is twofold:

1. Maximize TPV surface power density by maximizing transfer of convertible (high energy, above bandgap) photons from the radiator to the TPV diode.

2. Maximize TPV efficiency by minimizing transfer of non-convertible (low energy, below bandgap) photons from the radiator to the TPV diode.

Front surface spectral control performance is characterized by two key parameters: spectral efficiency and integrated above bandgap transmission efficiency. Spectral efficiency (shown in Equ. 3) is a direct multiplier on system conversion efficiency and is defined as the ratio of the above-bandgap power absorbed in the TPV cell active area to the total power absorbed over the same area (cell and filter). The integrated above-bandgap transmission of a filter (shown in Equ. 4) is proportional to the electrical output power density (W/cm^2) of the TPV module. Integrated above-bandgap transmission is defined as the ratio of the

electrical output power density from a TPV device with a filter to the electrical output power density that would be achieved with the same TPV device with a perfect anti-reflection coating (reflectivity $(\lambda,\theta)=0$).

$$\eta_{spectral} = \frac{\displaystyle\int_0^{\frac{\pi}{2}}\int_0^{\lambda_g} \varepsilon_{eff}(\lambda,\theta,T_{rad})\frac{T_{filter}(\lambda,\theta)}{1-R_{filter}(\lambda,\theta)}N(\lambda,T_{rad})\sin\theta\cos\theta\,d\lambda d\theta}{\displaystyle\int_0^{\frac{\pi}{2}}\int_0^{\infty}\varepsilon_{eff}(\lambda,\theta,T_{rad})N(\lambda,T_{rad})\sin\theta\cos\theta\,d\lambda d\theta} \qquad [Equ.3]$$

$$T_{>Eg} = \frac{\displaystyle\int_0^{\frac{\pi}{2}}\int_0^{\lambda_g} \varepsilon_{eff}(\lambda,\theta,T_{rad})\frac{T_{filter}(\lambda,\theta)}{1-R_{filter}(\lambda,\theta)}N(\lambda,T_{rad})\sin\theta\cos\theta\,d\lambda d\theta}{\displaystyle\int_0^{\frac{\pi}{2}}\int_0^{\lambda_g}\varepsilon_{rad}(\lambda,\theta,T_{rad})N(\lambda,T_{rad})\sin\theta\cos\theta\,d\lambda d\theta} \qquad [Equ.4]$$

where:

$T_{filter}(\lambda,\theta)$ is the filter Transmission versus wavelength and angle of incidence
$R_{filter}(\lambda,\theta)$ is the filter Reflection versus wavelength and angle of incidence
λ is wavelength
λ_g is the wavelength corresponding to the bandgap (E_g) of the TPV device
$N(\lambda,T_{rad})$ is Planck's blackbody spectral distribution of emissive power
θ is the angle of incidence (polar angle) of incoming photons
T_{rad} is the radiator temperature
$\varepsilon_{rad}(\lambda,\theta,T_{rad})$ is the radiator emissivity versus wavelength, angle and temperature
$\varepsilon_{eff}(\lambda,\theta,T_{rad})$ is the effective cavity emissivity calculated from:

$$\varepsilon_{eff}(\lambda,\theta,T_{rad}) = \frac{1}{\dfrac{1}{\varepsilon_{rad}(\lambda,\theta,T_{rad})}+\dfrac{1}{1-R_{filter}(\lambda,\theta)}-1} \qquad \left[Equ.5\right]$$

It is important to note that, because the radiator emits isotropically and is very close to the TPV modules, photons are incident on the filter surface with a polar angular distribution as shown in Figure 9. The angle-of-incidence (AOI) distribution for parallel flat plate geometry peaks at (and is symmetric about) 45 degrees. Therefore, front surface filters should be designed for optimum performance at 45° AOI and with

minimal sensitivity of filter performance to changes in AOI. Also, the angular characteristics of the filter (T_{filter} and R_{filter}) must be included in all performance modeling to achieve realistic results.

The front surface filter utilized in the system described in this paper is based on a tandem filter concept. As shown in Figure 10, the tandem filter concept is the combination of a plasma filter with an interference filter. The interference filter serves two purposes: first, it provides very high reflection of sub-bandgap photons in the 2.33 to ~6 micron range. Second, it "masks" a narrow absorption region (~4 microns) of the plasma filter. It is also worth noting that the interference filer can transition from highly transmissive to highly reflective over a very narrow (~0.1 micron) range which improves spectral performance.

The plasma filter is necessary because the interference filter's reflective range can not be extended past about 6 microns without impacting the transmission of the above-bandgap photons. At 950°C, about 17% of all radiant energy is emitted with a wavelength greater than 6 microns and the plasma filter is very effective at "recycling" this energy. Figure 11 shows how these two filters function together to produce a very effective spectral control technology.

Figure 2 shows the measured reflection versus wavelength our latest tandem filter at 45° AOI. As defined in Equ. 3, the spectral efficiency of this filter (based on measured data including angle of incidence effects) is ~79% and measured integrated above bandgap transmission of ~72 %. Furthermore, the same codes used to design this filter can predict filter performance with a high degree of accuracy. Figure 12 shows the measured performance of this filter design together with the pre-fabrication predictions. The predicted filter performance factor was 81%.

MODULE DESIGN & ASSEMBLY

Module design and assembly affects the η_{mod} term of equ.1. Recent improvements in module design and fabrication techniques have improved η_{mod} from <70% to >85%. Figure 13 provides a sketch of a current TPV module design. Module performance improvements, together with a description of the module design and/or assembly techniques that produced the performance improvements, are summarized as follows:

1) Reduced parasitic absorption of above bandgap energy
   Above bandgap energy is parasitically absorbed in non-active areas in the module including gold coated electrical interconnects and gaps between adjacent diodes. The energy incident on these surfaces is not available to convert to electricity and becomes waste heat. A significant reduction in parasitic absorption was achieved by moving the electrical busbar from the center of the diode to the edge of the diode (Figure 13). This produced a 7% increase in active area since the centerline busbar accounted for 10% of the diode area while the edge busbar reduced this to 3%. The reduction in busbar area is possible since moving the busbar from the center to the edge of the diode essentially changed the busbar from a point contact to a line contact which increased cross-sectional area by an order-of-magnitude. In addition to this increase in active area, the edge busbar also allowed the thickness of the electrical interconnects to be reduced from 63um to 13um. This low profile interconnect reduced the gap between adjacent diodes, further reducing parasitic losses.

2) Improved electrical networking performance
   An electrical networking model was developed to conduct parameter studies that identified the key diode electrical properties contributing to networking losses. The multi-chip module (MCM) approach (Figure 13) allows the selective assembly of diodes into modules which can reduce networking losses. Lockheed Martin is currently working to adapt the quaternary material system to a monolithic integrated module (MIM) system which could promote mass fabrication of modules. A second item that improved module electrical performance was changing the assembly technique used to attach the electrical interconnects to the diode busbar. Microwelding, a direct bond technique (i.e., gold-to-gold), replaced a solder technique. This eliminated a consistent degradation to diode shunt resistance, which in turn had reduced module electrical fill factor by 5% when compared to diode fill factor. Currently, there is no measurable degradation in diode performance when assembled into a module.

6

3) Improved yield

The primary increase in yield was achieved by using the direct bond technique for the diode front-surface electrical interconnects discussed above. This eliminated a reduction in yield associated with solder shorting the PN junction along the edge of the diode, below the diode busbar.

In summary, significant improvement in TPV module performance was achieved by minimizing performance losses associated with TPV module design and assembly. While only small, flat modules (i.e., $1cm^2$ and $4cm^2$) are currently being fabricated to support efficiency testing, both flat plate and cylindrical modules have been fabricated, the largest of which produced 400W of electric power.

EFFICIENCY MEASUREMENTS

Other than building and testing full-scale systems, the most reliable determinations of TPV conversion efficiency are derived from direct measurements of small integrated module specimens tested under prototypic conditions. Measurements of conversion efficiency report here are based on such measurements carried out on small (1-4cm^2) specimens comprised of all components found in full-scale units. Unlike photovoltaic systems, TPV systems measure efficiency based on the total absorbed power rather than in the incident power:

$$\eta_{TPV} = \frac{P_{max}}{\dot{Q}_{meas}}$$
(Equ. 6)

where: P_{max} is the peak (load matched) power output
Q_{meas} is the total absorbed power

The Photonic Cavity Test (PCT) System is shown in Figure 3. It was developed to provide an optically prototypic environment in which the performance of small modules would accurately mimic the behavior of larger-scale units. To achieve this end, the test system:

Models the flat-plate geometry we envision for larger units
Includes a large, graybody radiator (SiC)
Explicitly incorporates geometric effects, isotropic incident radiation, photonic recycling
Is run at prototypic radiator and diode temperatures

Furthermore, all testing was carried out under vacuum conditions to improve the reliability of the results by eliminating spurious convective heat loss mechanisms. Modules were tested in the PCT system under steady-state conditions. The maximum power point was determined from the module I-V curve. Figure 14 is a typical I-V curve. The heat absorption rate was measured from the temperature gradient developed in the copper pedestal to which the module is bonded (see Fig. 3). Measured conversion efficiency is the ratio of these two terms.

The major non-prototypic characteristic of the PCT is the "gold shield enhancement effect". Because the small module is surrounded by highly reflective shields (rather that other modules), the incident radiation and the measured power density are artificially increased. Detailed monte carlo and ray tracing analyses have shown that this effect increases power by 8%. Effects on measured efficiency are small. All power density values reported here have been reduced by 8% to account for the "gold shield enhancement effect".

Figure 15 presents the results of efficiency measurements and Figure 16 shows the measured power density results for two recent TPV modules. Table 2 provides more detailed information in tabular format. Module #25 was a $1cm^2$ specimen with two diodes (in series) and a front surface filter for spectral control. Module #47 was a $4cm^2$ specimen with eight diodes (series/parallel configuration) of similar design.

TABLE 2 – Results of Measurements in Photonic Cavity Test (PCT) System Lockheed Martin TPV Modules #25 and #47		
Parameter	**Module #25**	**Module #47**
Dimensions	1cm X 1cm	1.89cm X 1.99cm
Radiator Temp (C)	953	956
Diode Temp (C)	23	22
Open Circuit Voltage (V/diode)	0.306	0.311
Short Circuit Current (A/cm^2)	2.737	2.400
Fill Factor	0.693	0.693
Elect. Power Output (W/cm^2) (corr. for shield enhancement effect)	0.534	0.510
Absorbed Power (W/cm^2) (corr. for shield enhancement effect)	2.76	2.61
Measured Conversion Efficiency	19.3%	19.5%

PERFORMANCE MODELING

The performance of the TPV modules was predicted using in-house codes which are based on well known principles of semiconductor materials and optical behavior. These codes have been extensively benchmarked against small-scale testing of TPV hardware under prototypic conditions (Ref. 6). The calculations include detailed characterization data from each component and corrections for the complex behavior of the photonic cavity.

Geometric effects (surface structures, etc.) are modeled as simple area fractions; detailed 3-dimensional modeling is not included. Furthermore, angular-dependent effects (emissivity, reflectivity) are modeled with energy-weighted average values. Finally, the models incorporate an 8% radiation enhancement factor to account for the second-order effect of the gold shields which surround the TPV module. This effect is an artifice of the PCT test configuration and will not occur in a full-scale TPV unit.

Figure 4 is a comparison of the in-cavity test performance of several recent modules to the modeling predictions. As shown, these models routinely predict test results to about +/- 2%.

EFFECT OF DIODE TEMPERATURE ON TPV CONVERSION EFFICIENCY

The performance of the TPV modules is dependent on the temperature at which the diodes operate. At higher temperatures, the open circuit voltage and the fill factor will suffer primarily due to an increase in reverse (dark) current. Complicating the matter, the diode bandgap will shift to longer wavelengths which can disturb the compatibility between bandgap and filter "turn-on" wavelength. Figure 17 shows the sensitivity of efficiency to diode temperature for a recent Lockheed Martin module.

References

1. 'Silicon Photovoltaic Cells in TPV Conversion'; USAEC Contract AT(30-1)-3587; March 10, 1967

2. RM Swanson; 'Final Report, Radiant Energy Conversion'; ER-1272 EPRI Research Project 790-2; December, 1979

3. JC Bass, NB Elsner, PH Miller; 'Nuclear Thermophotovoltaics'; 18th IECEC Conf.; July, 1983

4. G.W. Charache, J.L. Egley, D.M. DePoy, L.R. Danielson, M.J. Freeman, R.J. Dziendziel, J.F. Moynihan, P.F. Baldasaro, B.C. Campbell, C.A. Wang, H.K. Choi, G.W. Turner, S.J. Wojtczuk, P. Colter, P. Sharps, M. Timmons, R.E. Fahey, K. Zhang, 'Infrared Materials for Thermophotovoltaic Applications,' J. Electron. Mater. 27, 1038-1042 (1998).

5. PF Baldasaro, EJ Brown, DM DePoy, BC Campbell, JR Parrington; "Experimental Assessment of Low Temperature Voltaic Energy Conversion"; First NREL Conference on Thermophotovoltaic Generation of Electricity; July, 1994

6. EJ Brown, CT Ballinger, GW Charache, LR Danielson, DM DePoy, TJ Donovan, M LoCasio; "Measurements of Conversion Efficiency for a Flat Plate Thermophotovoltaic System Using a Photonic Cavity Test System"; AIAA-2000-3029, The 35th IECEC Conf., Las Vegas, NV; July, 2000

FIGURE 1 - Measured TPV Conversion Efficiency at Lockheed Martin Corp.
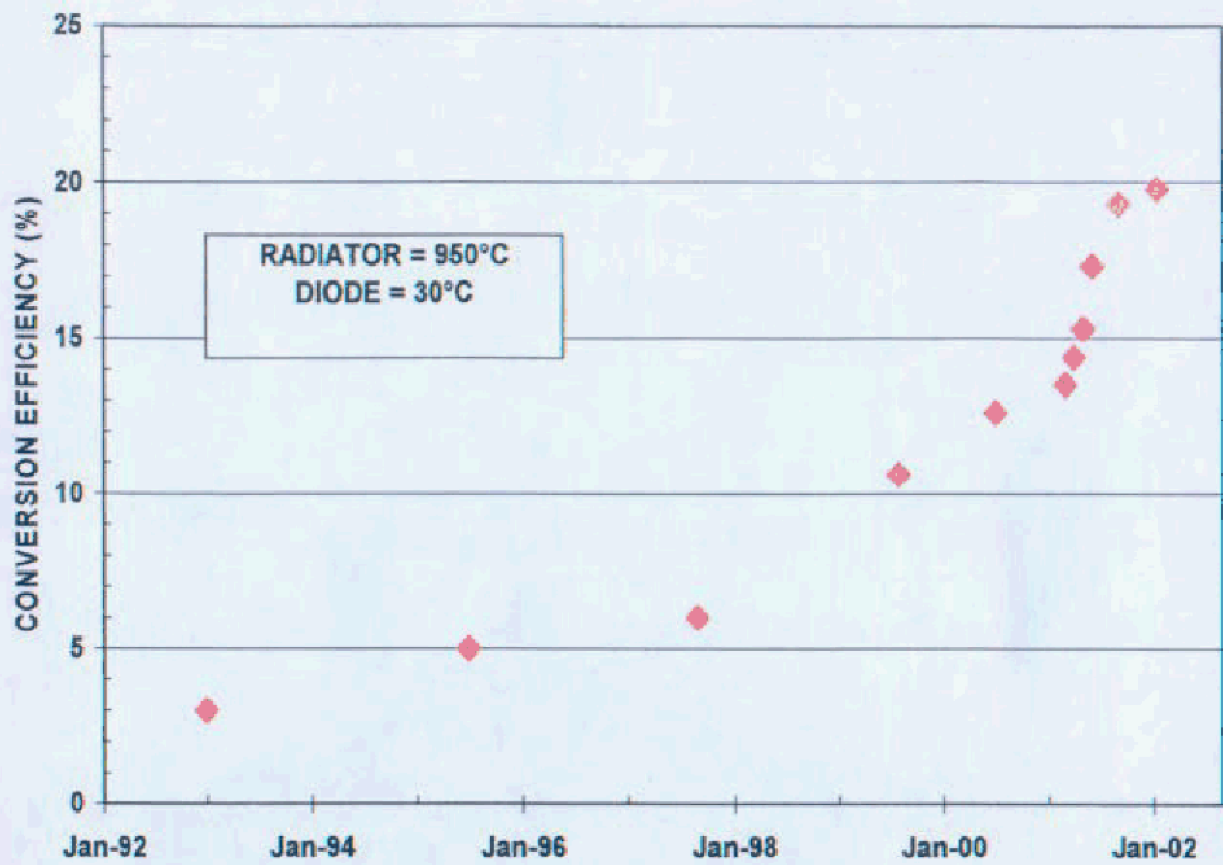
RADIATOR = 950°C
DIODE = 30°C

FIGURE 2 - Measured Reflectivity Performance
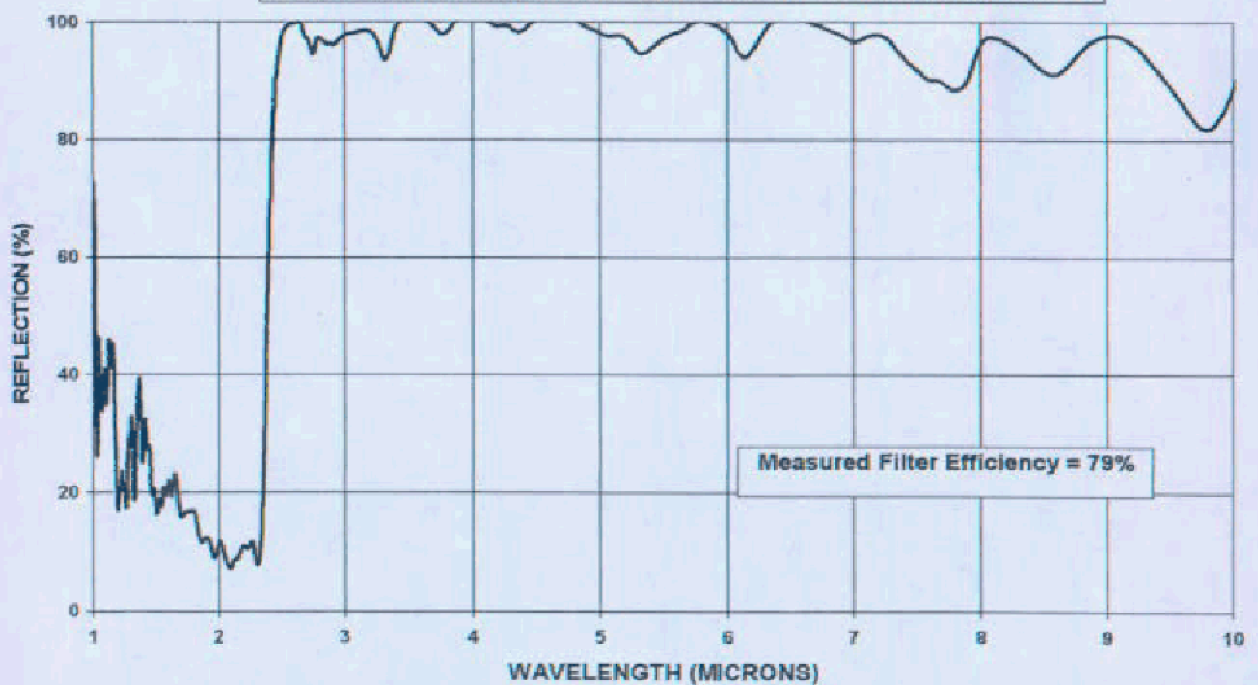Lockheed Martin Tandem Filter Matched to 0.52 eV (2.38 micron) Diodes

Measured Filter Efficiency = 79%

FIGURE 3 – Photonic Cavity Test (PCT) System

BORELECTRIC HEATERS

RADIATOR

GOLD SHIELDS

Elect. Power Output

MODULE -
DIODES & FILTER

Q_{reject}

PEDESTAL
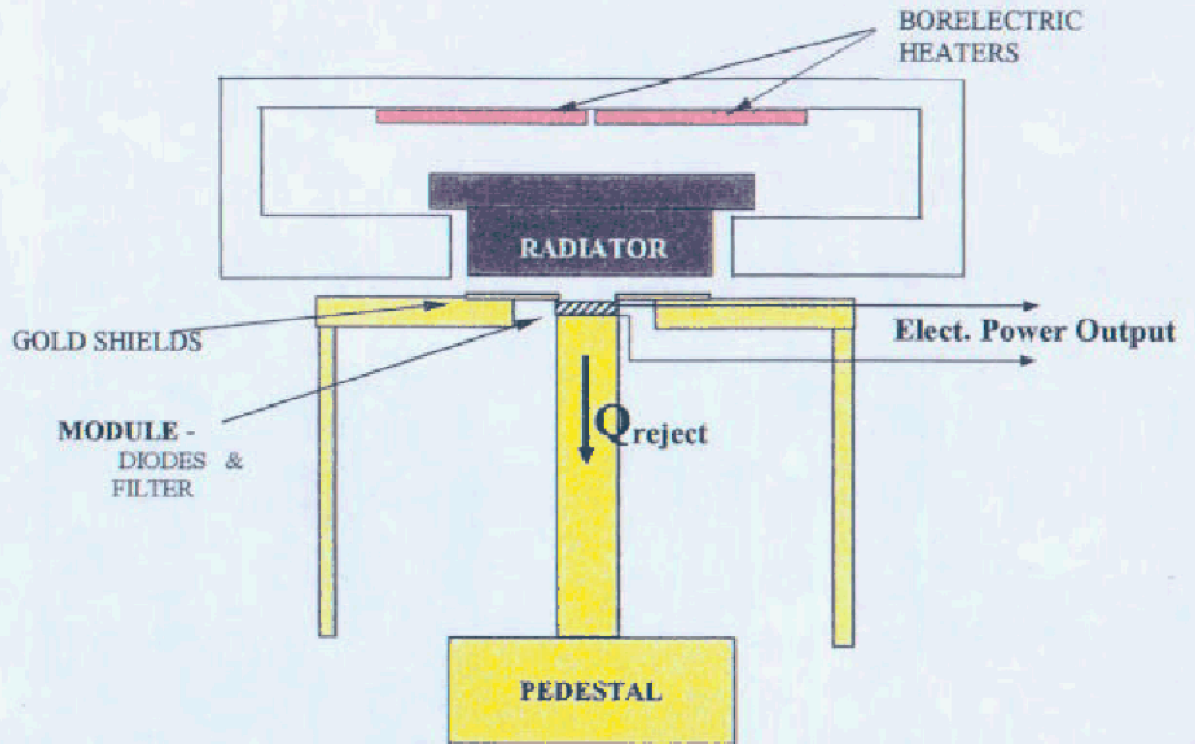
FIGURE 4 - In-Cavity Benchmarking of TPV Computational Model
Conversion Efficiency vs. Hot-side Temperature

MODELING PREDICTIONS   IN-CAVITY MEASUREMENTS

MODULE #25

MODULE #40

MODULE #17

MODULE #4

Conversion Efficiency (%)

Radiator Temperature (°C)
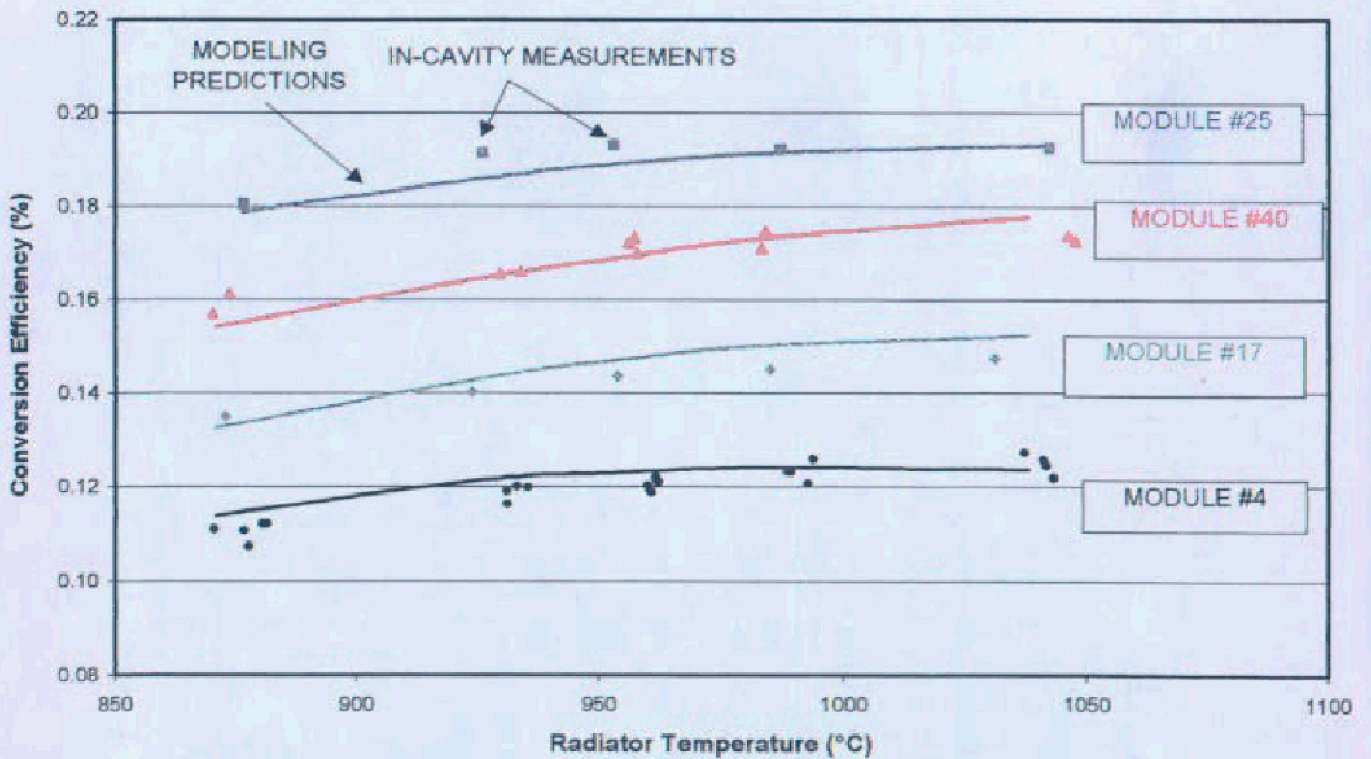
FIGURE 5- TPV direct energy conversion system with front surface filter for spectral control

RADIATOR

RADIANT SPECTRUM

LOW ENERGY PHOTONS

HIGH ENERGY PHOTONS

LOAD

SPECTRAL FILTER
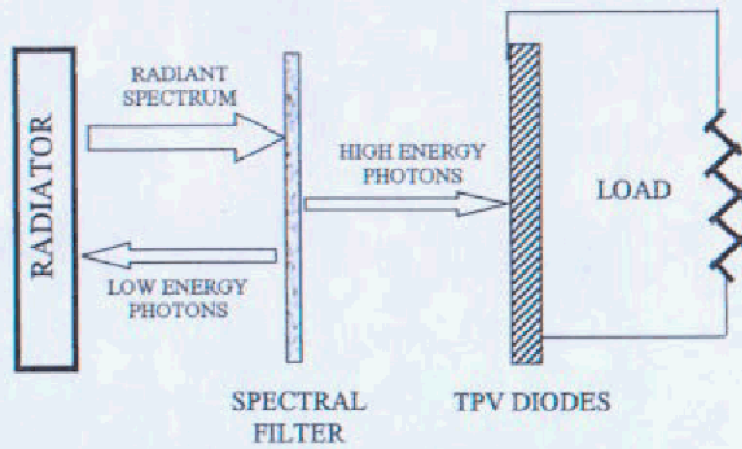
TPV DIODES

Figure 6 - Convertible Portion of a Blackbody Radiant Spectrum by a TPV Diode

CONVERTIBLE ENERGY
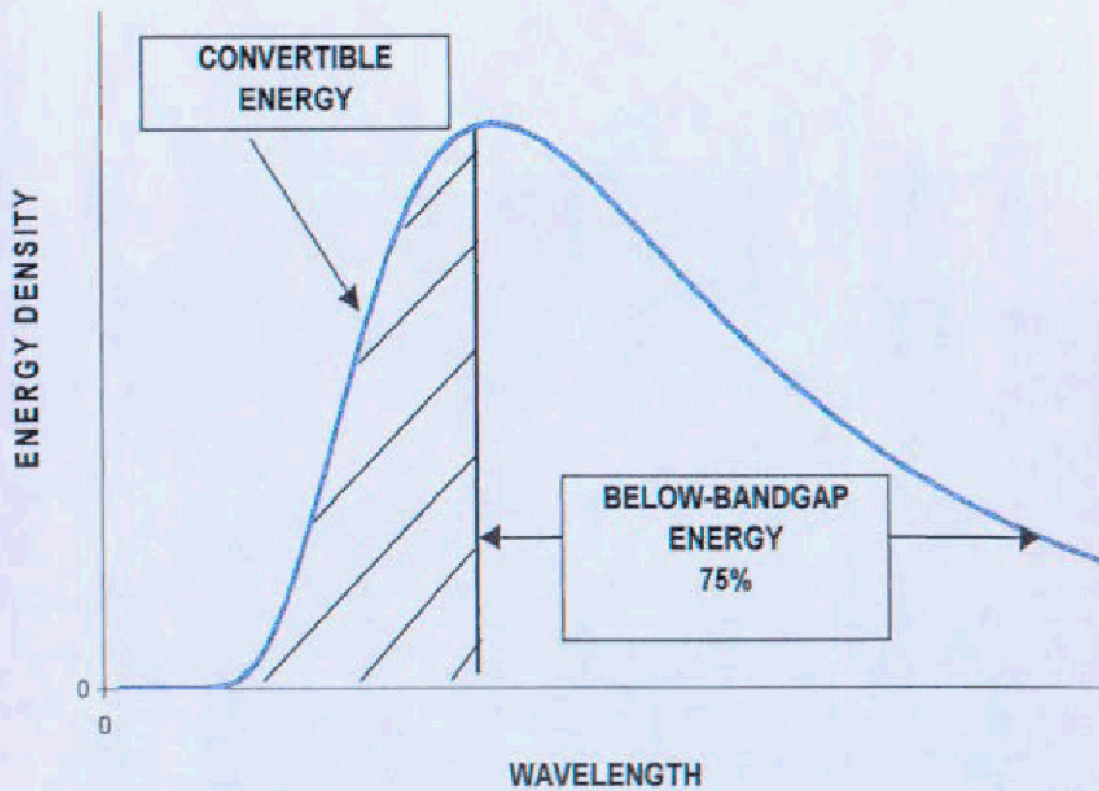
ENERGY DENSITY

BELOW-BANDGAP ENERGY 75%

0

0

WAVELENGTH

## FIGURE 7 - TPV System Efficiency and Power Density vs. Diode Bandgap

Legend:
- TPV Efficiency
- TPV Surface Power Density

$T_{radiator}$ = 925 C
T_{diode} = 55 C
Below Bandgap Reflectivity = 97%

X-axis: Eg (eV)
Left Y-axis: TPV Efficiency (%)
Right Y-axis: TPV Surface Power Density (W/cm2)
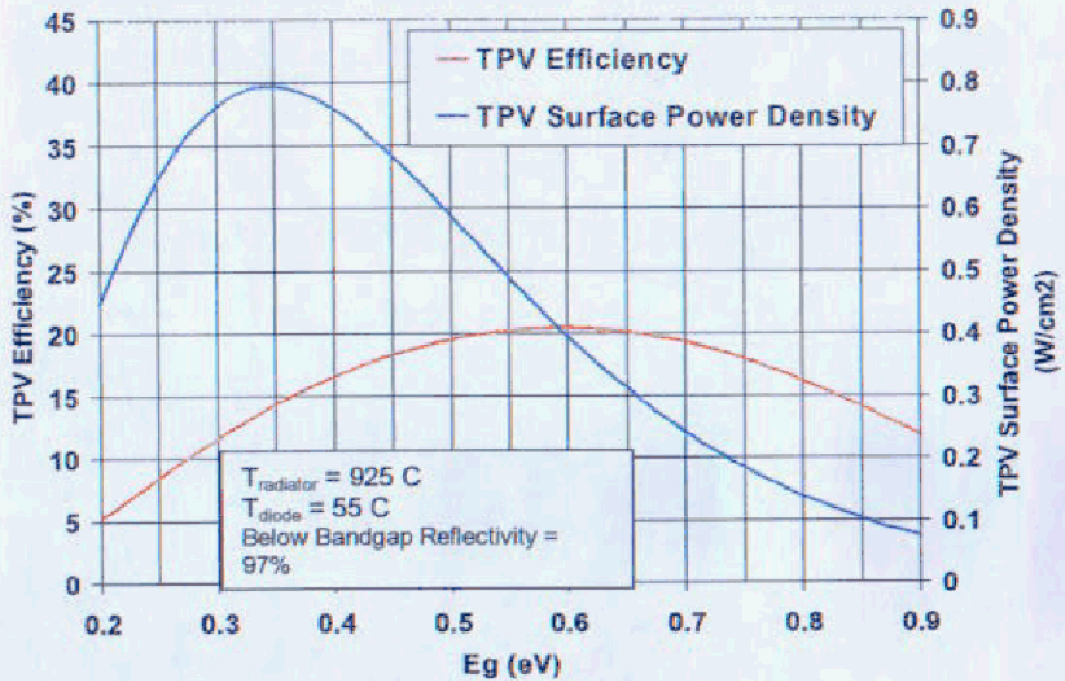
FIGURE 8 – GaInAsSb TPV Device Layers with Metal Contacts

front contact metal grids

- p – GaSb — contact
- p - AlGaAsSb — window
- p - GaInAsSb — emitter
- n - GaInAsSb — base
- n - GaSb — substrate
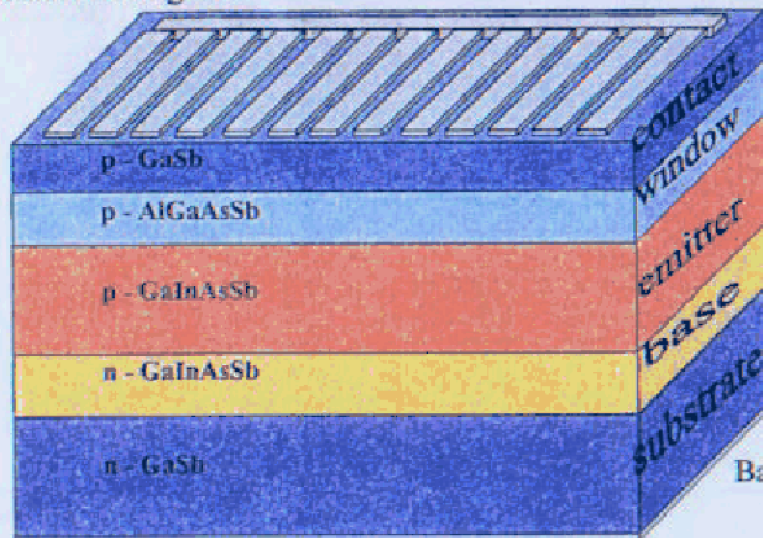
Back metal contact

FIGURE 9 - Angle of Incidence Considerations for TPV Spectral Control
Photon Distribution as a function of Angle of Incidence for Infinite Parallel Flat Plate Geometry
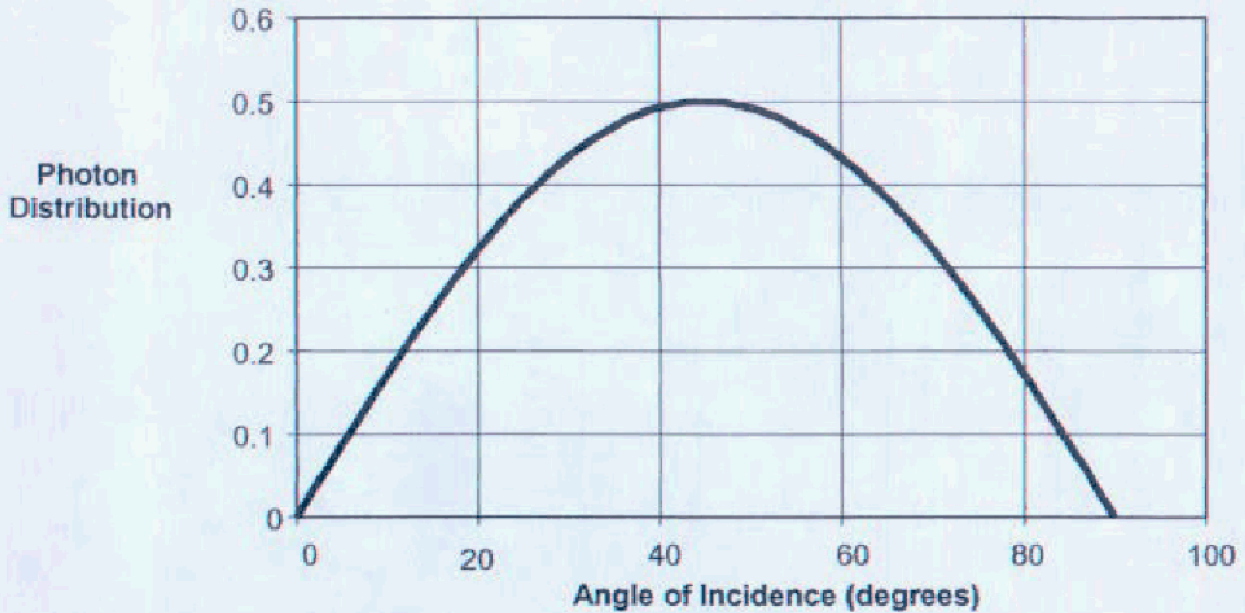
Filters Must be Designed for 45 degree Angle of Incidence
Filters Must be Designed to Minimize Off Design Angle Performance

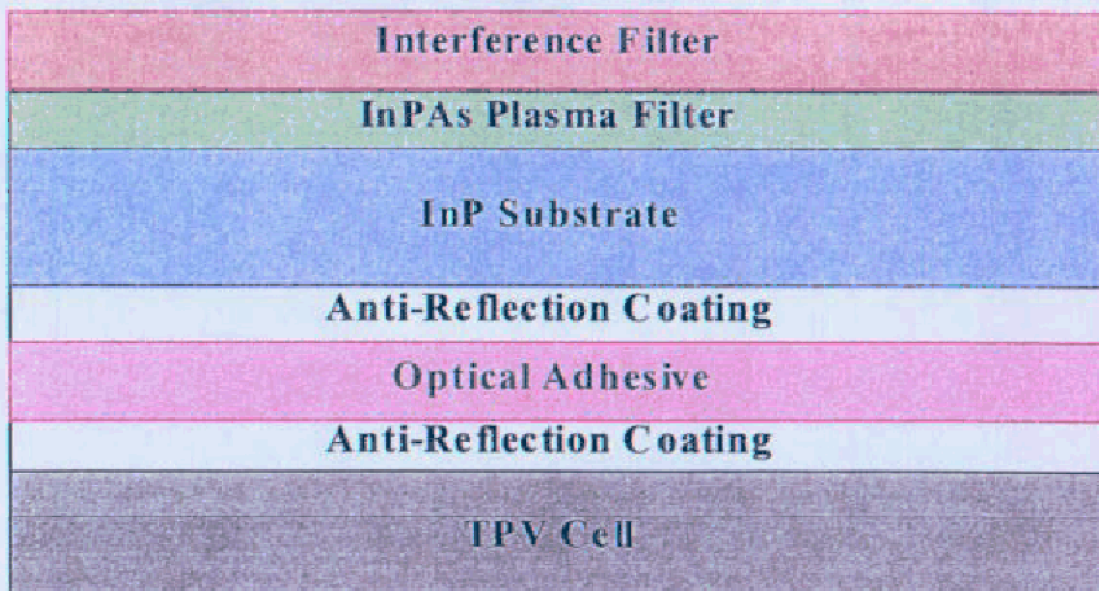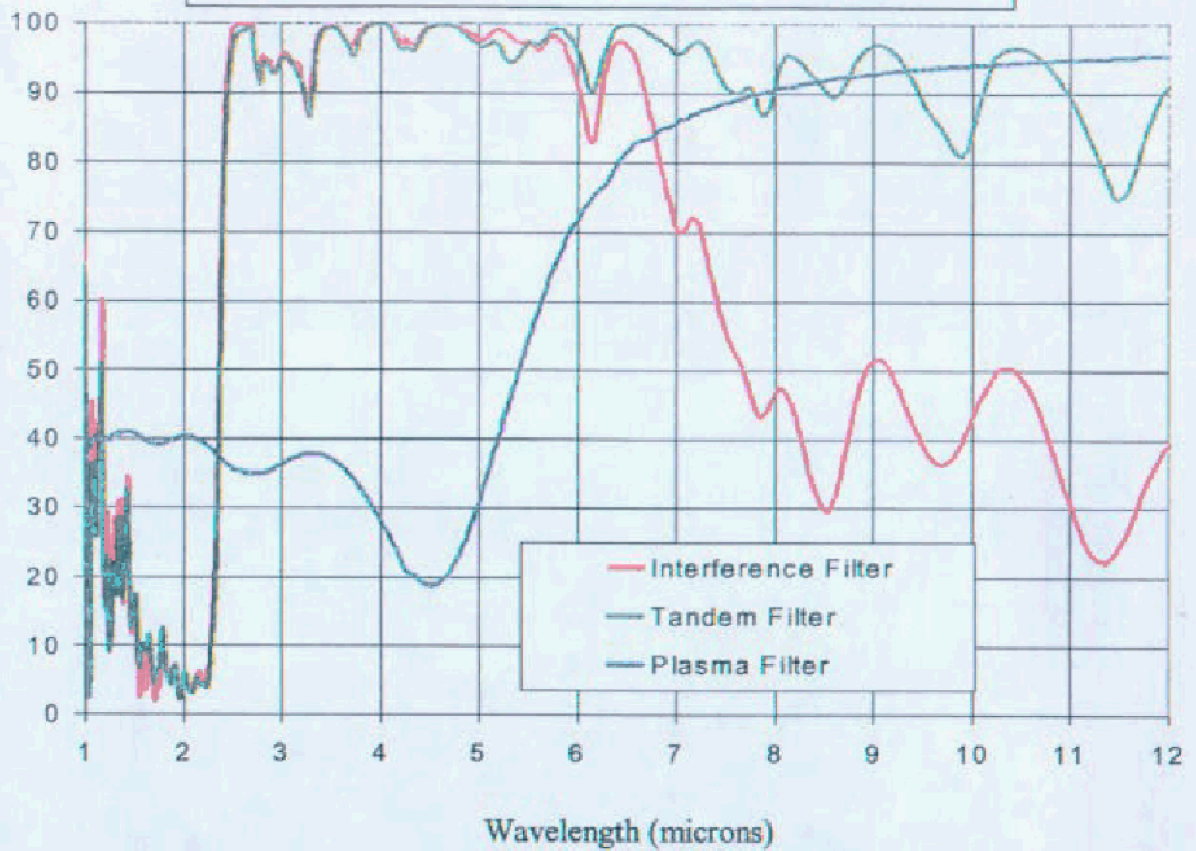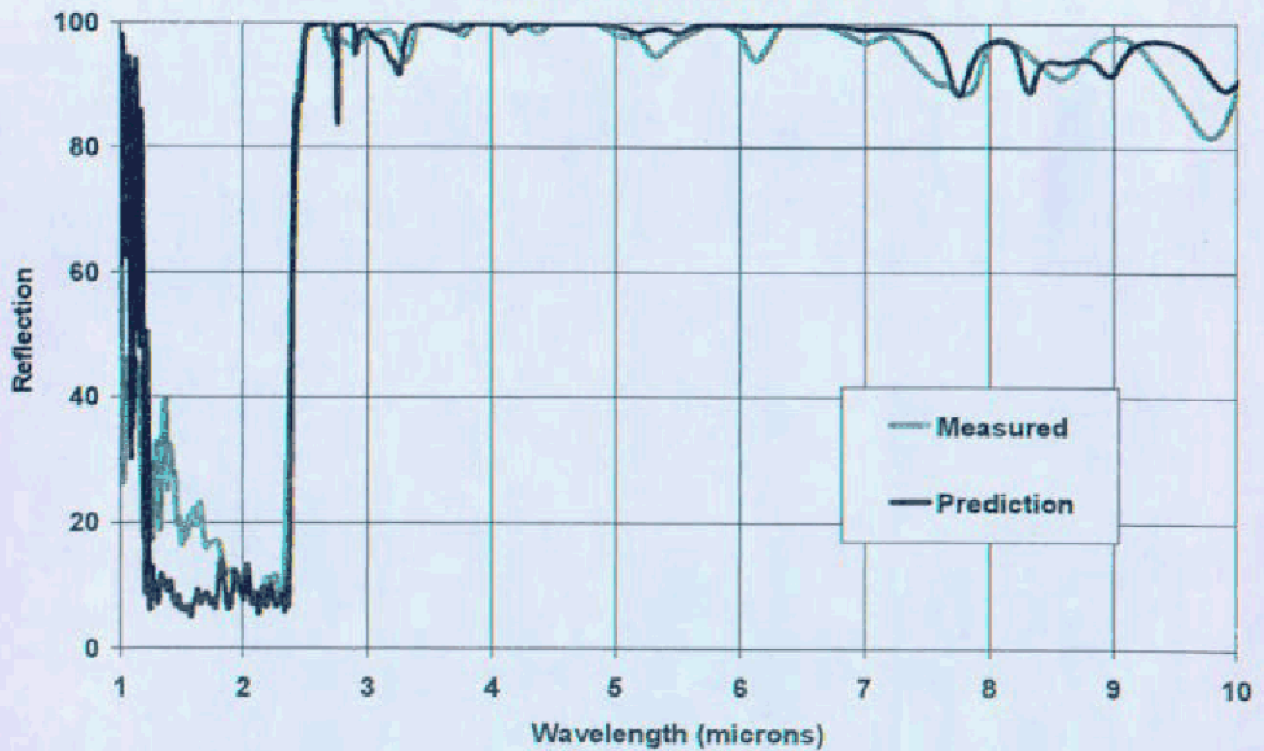FIGURE 10 - Tandem Filter Concept

| Interference Filter |
| InPAs Plasma Filter |
| InP Substrate |
| Anti-Reflection Coating |
| Optical Adhesive |
| Anti-Reflection Coating |
| TPV Cell |

FIGURE 11 - Tandem Filter Reflectvity

Wavelength (microns)

FIGURE 12 - Comparison of Measurementsand Predictions for Lockheed Martin Tandem Filter

Wavelength (microns)

15

Gridlines

Busbar

TPV Diode

AlN Substrate

Electric Power Lead   Electrical Interconnect   Metallization

Electrical
Interconnect

Busbar

AlN Substrate

Electric Power Lead   Metallization
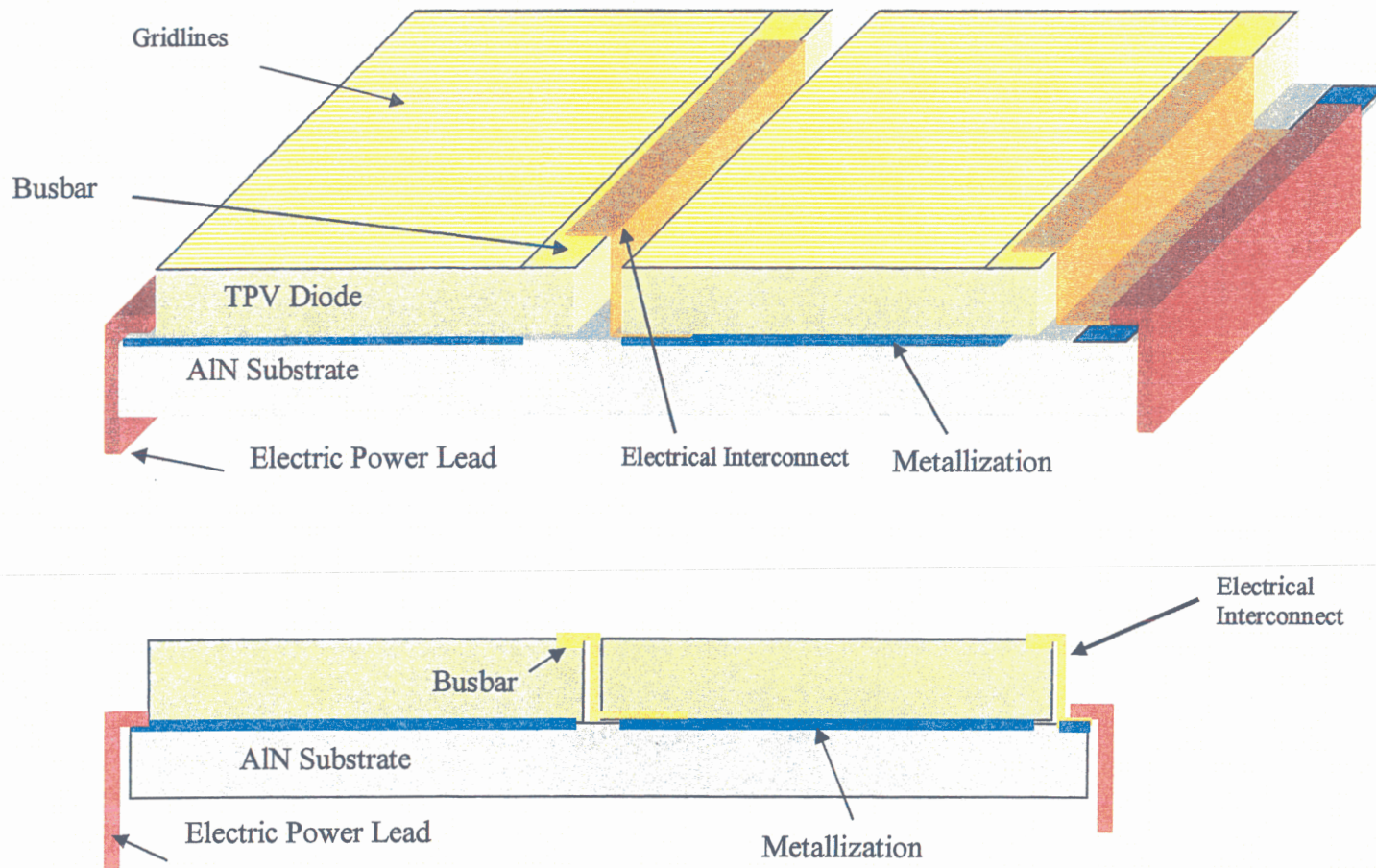
Figure 13. TPV Power Module Sketch
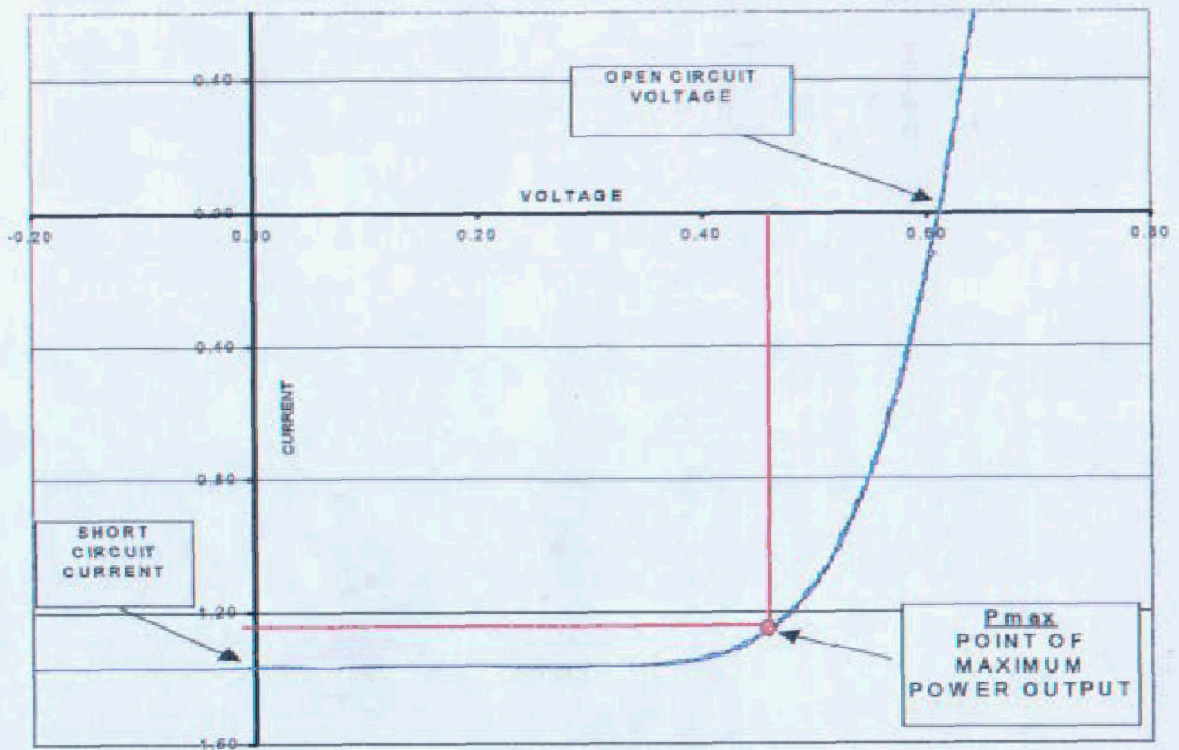
FIGURE 14 - Typical TPV I-V Curve

FIGURE 15 - PCT Measurements of Lockheed Martin TPV Modules
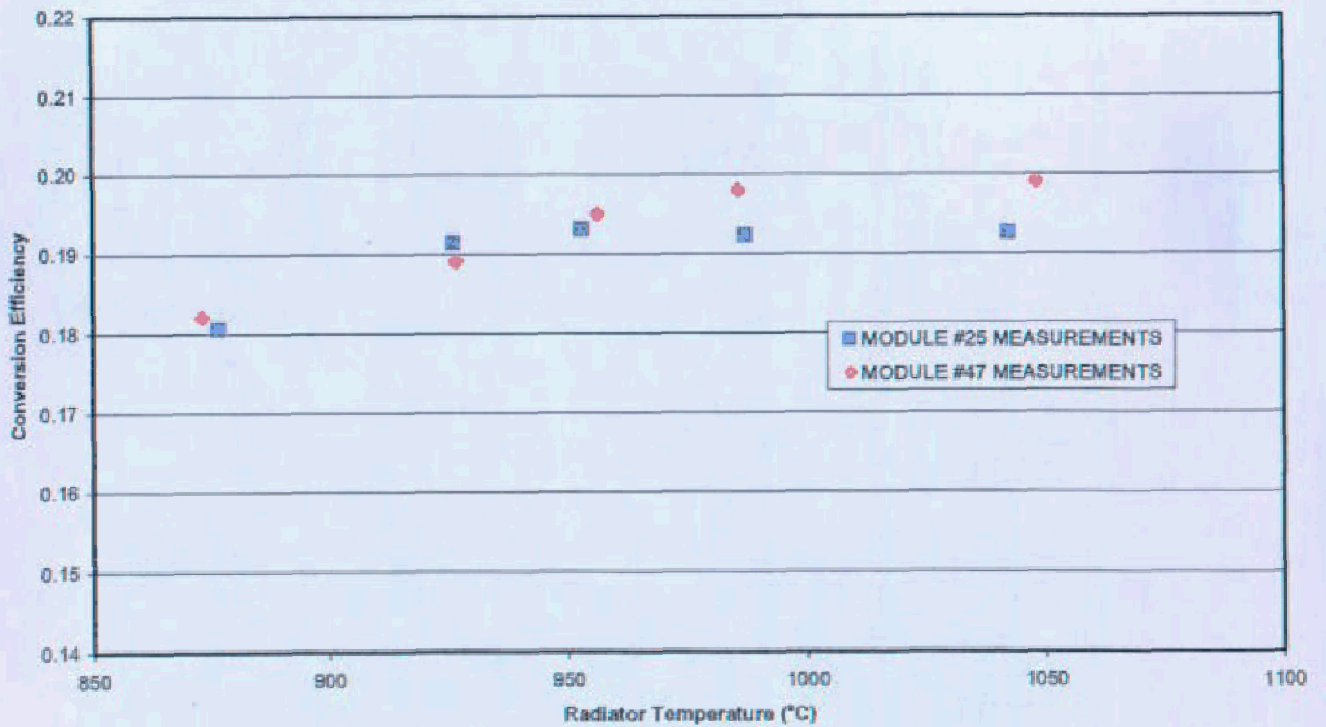Conversion Efficiency vs Radiator Temperature

FIGURE 16 - PCT Measurements of Lockheed Martin TPV Modules Power Density vs Radiator Temperature

■ MODULE #25 MEASUREMENTS
● MODULE #47 MEASUREMENTS

CORRECTED FOR SHIELD ENHANCEMENT EFFECT

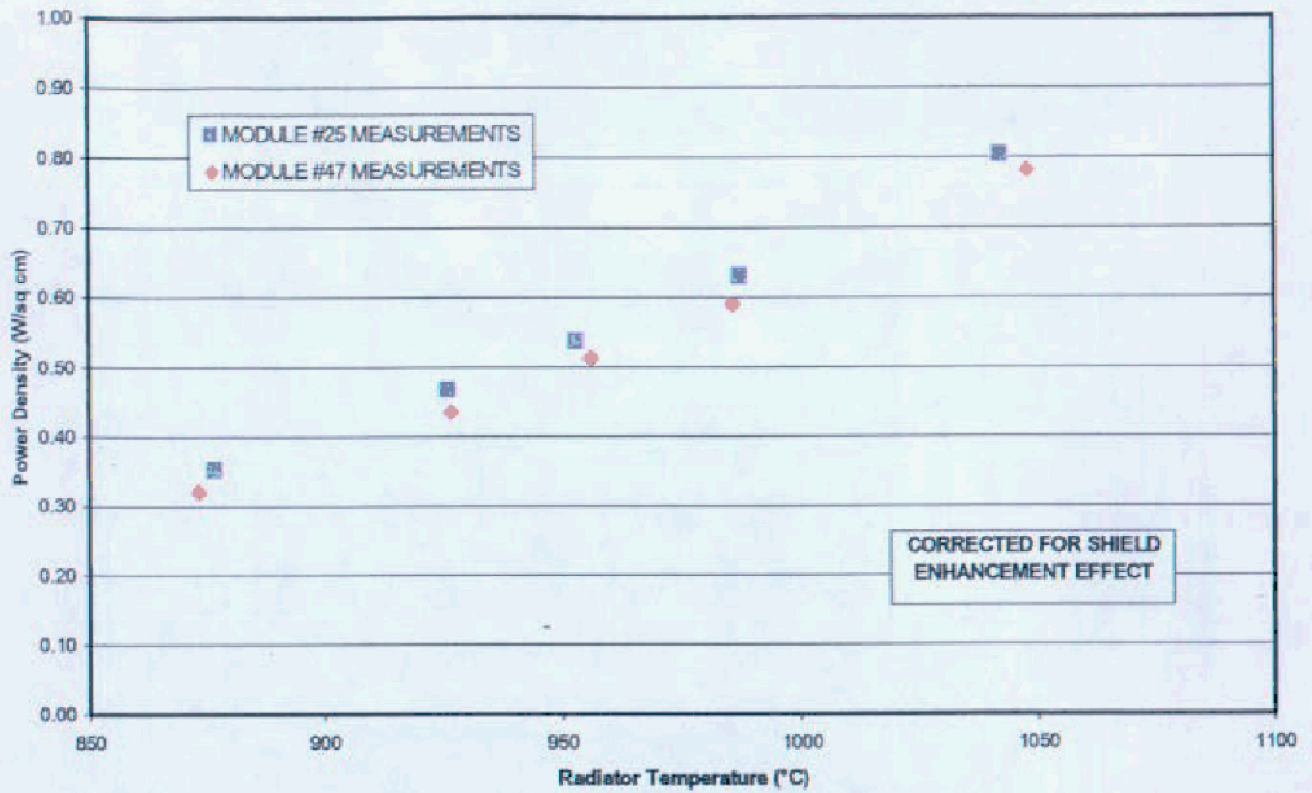Power Density (W/sq cm) vs Radiator Temperature (°C)

FIGURE 17 - Effect of Diode Temperature on TPV Conversion Efficiency

LOCKHEED MARTIN
TPV MODULE #25
(RADIATOR = 950°C)

Conversion Efficiency vs Diode Temperature (°C)